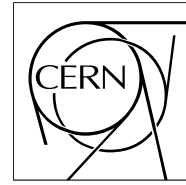


**The Compact Muon Solenoid Experiment**

# **CMS Note**

Mailing address: CMS CERN, CH-1211 GENEVA 23, Switzerland



**9 November 2000**

## **Isolated Muon Trigger**

C. Albajar<sup>1)</sup>

*Universidad Autonoma de Madrid, Madrid, Spain*

G. Wrochna<sup>2)</sup>

*Soltan Institute for Nuclear Studies, Warsaw, Poland*

### **Abstract**

An Isolated Muon Level 1 Trigger is proposed to reject muons from decays of  $b$  and  $c$ -quarks preserving high efficiency for muons from heavier objects. It is shown that the proposed algorithm is feasible and significant rejection factor (3-10) can be achieved. A similar algorithm can be applied at High Level Triggers.

---

<sup>1)</sup> Partially supported by CICYT (Spain) under grant AEN99-0571.

<sup>2)</sup> Partially supported by the Polish Committee for Scientific Research under grant KBN 621/E-78/SPUB/P-03/DZ 5/99.

# 1 Physics motivation

One of the main backgrounds for the muon trigger at LHC are decays of  $b$ - and  $c$ -quarks. They dominate single and double muon rate over wide range of transverse momentum  $p_t$  values (see Table 1). The effect is even more pronounced after the First Level Trigger (L1), because of its finite momentum resolution.

	dominant particle rate		dominant L1 trigger rate	
	$p_T$ range	$\mu$ source	$p_T$ range	$\mu$ source
1 $\mu$	1-4 GeV	$\pi, K$	1-4 GeV	$\pi, K$
	4-30 GeV	$b, c$	> 4 GeV	$b, c$
	> 30 GeV	$W$		
2 $\mu$	< 15 GeV	$b, c$	< 30 GeV	$b, c$
	> 15 GeV	$Z^0$	> 30 GeV	$Z^0$

Table 1: Dominant single and double muon rates for various  $p_T$  intervals.

It is very difficult to reject this background, because these are real muons, pointing to the interaction vertex, often having rather high momentum. The only difference, compared to muons from decays of  $W$ -boson or new heavy objects is, that muons from  $b$  and  $c$  decays are produced inside jets. This property can be exploited by the trigger. It can be checked whether a muon is surrounded by hadrons. The aim of the present study is to define isolation criterion, that are possible to implement at the First Level Trigger, and to simulate its performance.

The subject is difficult, because it involves a combination of calorimeter and muon trigger data. It requires detailed simulation of jet development, calorimeter response and muon trigger algorithms. Preliminary results were obtained in 1996 with a simplified simulation [1]. The results were encouraging and the study was continued with a full detail GEANT/CMSIM simulation [3]. It is described in the following sections.

## 2 The algorithm

An isolated muon trigger algorithm should check whether there was a significant energy deposit in a calorimeter around a given muon. The muon can be considered as isolated if the energy in a certain window is lower than a threshold. The threshold value should be optimised for a high signal to background ratio.

A possible implementation of the isolated muon trigger at L1 should involve both calorimeter and muon trigger processors. The Calorimeter Trigger operates in *regions* of  $\Delta\eta \times \Delta\phi = 0.35 \times 0.35$ . A *quiet bit* is assigned to each region and it is set if the transverse energy  $E_T$  deposited in this region is below a threshold.

The Muon Trigger provides a list of up to 4 muon candidates. For each candidate its  $p_t$ ,  $\eta$  and  $\phi$  is given. The Global Trigger can use this information to find the corresponding calorimeter region and check whether the quiet bit is set or not. If the region is *quiet* the muon is labelled *isolated*.

One calorimeter region is too small to contain an entire jet. Therefore we also consider algorithms based on information from several regions. For this purpose one has to combine quiet bits from several regions. The muon is isolated if **all** the regions in the window around it are quiet. We consider four window sizes:

- $\Delta\eta \times \Delta\phi = 1 \times 1$  regions
- $\Delta\eta \times \Delta\phi = 1 \times 2$  regions
- $\Delta\eta \times \Delta\phi = 2 \times 2$  regions
- $\Delta\eta \times \Delta\phi = 3 \times 3$  regions

The algorithms described above are illustrated in Fig. 1.

## 3 Simulation

Two physics processes were chosen to represent the signal: inclusive  $W$  production and supersymmetric  $A^0$  higgs boson production. The mass of the  $A^0$  was set to 200 GeV. For the background we considered the most difficult case, namely the  $b\bar{b}$  pairs. Both signal and background events were generated with PYTHIA 5.7 [2]. Simulated production mechanisms for  $W$  and  $A^0$  are given in Table 2. Four  $b\bar{b}$  samples were produced with different cuts on colliding partons and muons (see Table 2). The  $W$  and  $A^0$  bosons, as well as  $B$  mesons, were forced to decay into muons.

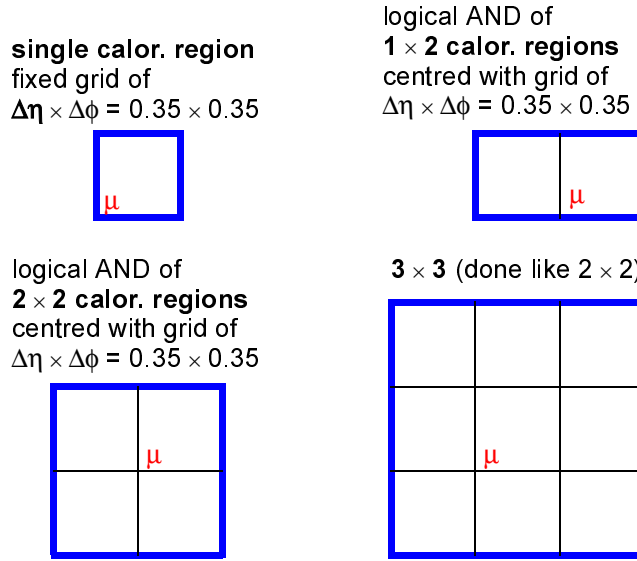


Figure 1: Various isolated muon trigger algorithms.

W production		A <sup>0</sup> production		b $\bar{b}$ production		
$\sigma = 4.8 \cdot 10^{-05}$ mb		$\sigma = 3.0 \cdot 10^{-12}$ mb		MSEL=5		
process	MSUB	process	MSUB	$\hat{p}_T >$	$p_T^\mu >$	$\sigma$
$f_i \bar{f}_j \rightarrow W^\pm$	2	$f \bar{f} \rightarrow A^0$	156	10 GeV	5 GeV	$1.73 \cdot 10^{-02}$ mb
$f_i \bar{f}_j \rightarrow gW^\pm$	16	$q \bar{q} \rightarrow A^0$	157	30 GeV	15 GeV	$5.53 \cdot 10^{-04}$ mb
$f_i \bar{f}_j \rightarrow \gamma W^\pm$	20	$g \bar{g} \rightarrow q \bar{q} A^0$	186	40 GeV	20 GeV	$1.95 \cdot 10^{-04}$ mb
$f_i g \rightarrow f_k W^\pm$	31	$q \bar{q} \rightarrow q \bar{q} A^0$	187	50 GeV	25 GeV	$8.49 \cdot 10^{-05}$ mb
$f_i \gamma \rightarrow f_k W^\pm$	36					

Table 2: Simulated processes ( $f$  stands for fermions).

The detector response was simulated with CMSIM 114 [3]. Only the barrel calorimeter was used, which extends up to  $|\eta| = 1.5$ . In order to contain the sliding isolation window in the barrel we have used only muons with  $|\eta| < 1.055$ . Each generated sample was passed through the detector twice for two different luminosities. For  $\mathcal{L} = 10^{34} \text{cm}^{-2} \text{s}^{-1}$  a number of pileup events were superimposed (25 on average), whereas for  $\mathcal{L} = 10^{33} \text{cm}^{-2} \text{s}^{-1}$  no pileup was added.

## 4 Results

The muon  $p_T$  spectra for both signal and background are shown in Fig. 2. The distribution of energy deposited in the calorimeters around the muon track is given in Fig. 3 for different cone radii  $R = \sqrt{(\Delta\eta)^2 + (\Delta\phi)^2}$ . One can see that the energy around muons from W and A<sup>0</sup> decays is small and it is well concentrated. In the case of b $\bar{b}$  events the energy deposited around the muon is much larger and distributed widely.

The trigger hardware can only look at calorimeter regions of  $\Delta\eta \times \Delta\phi = 0.35 \times 0.35$ . We have considered algorithms based on  $1 \times 1$ ,  $1 \times 2$ ,  $2 \times 2$  and  $3 \times 3$  regions. The muon is labeled as *isolated* if the energy deposited in each of 1, 2, 3 or 9 regions is below the threshold. This is equivalent to taking the maximum energy among all considered regions and comparing it with the threshold. The distribution of this maximum energy for the four algorithms is shown in Fig. 4 for low and high luminosity.

There are two important parameters of the algorithms to be optimised: energy threshold and the size of the isolation window. Too low a threshold would remove too much signal, whereas too high a threshold would accept too much background. Window area much smaller than a typical jet size makes the background indistinguishable from signal. A large window size causes accumulation of noise and pileup energy which may mimic a jet. All these dependences can be seen in Figs 5 and 6 which show the fraction of accepted signal and background events as a function of the energy threshold for different window sizes at low and high luminosity. For the case of  $A \rightarrow \mu\mu$  decays the efficiency is calculated for each muon independently.

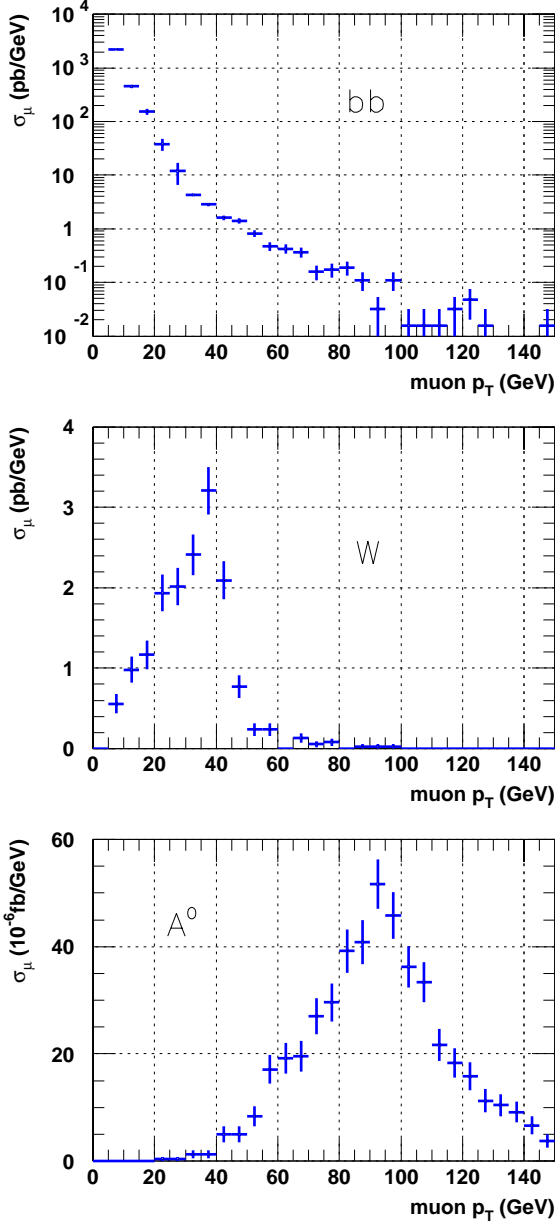


Figure 2: Muon  $p_T$  spectra.

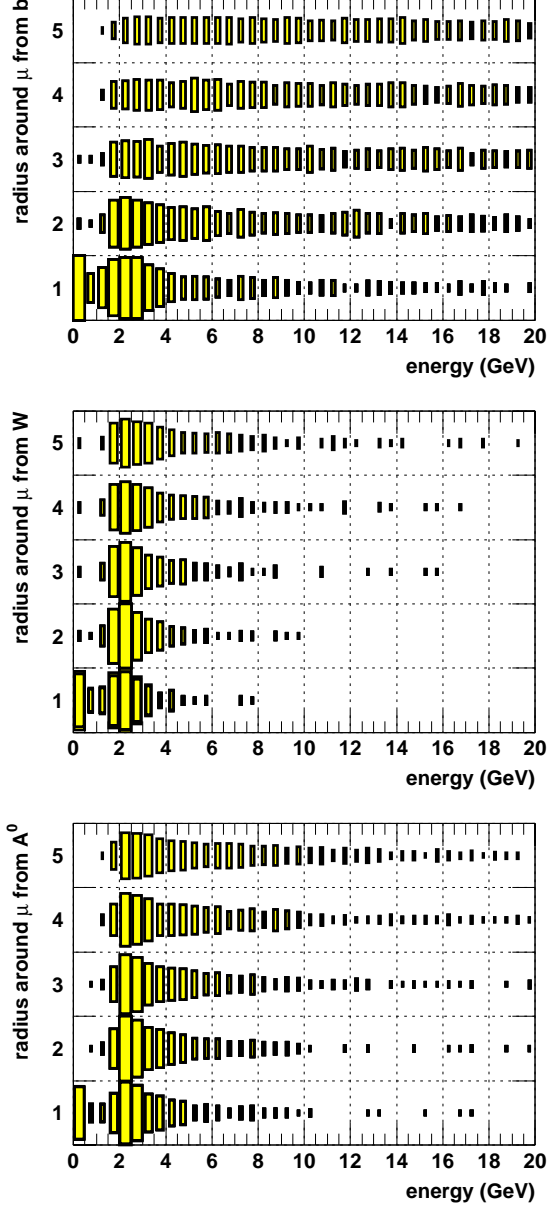


Figure 3: Distribution of energy deposited in a cone of radius  $R = \sqrt{(\Delta\eta)^2 + (\Delta\phi)^2}$  around a muon.

As an example of possible settings for the isolation algorithm we have chosen the energy threshold such that it preserves 90 % efficiency for the  $A^0$  muons. This usually corresponds to  $>95$  % efficiency for muons from  $W$  decays. The threshold values are given in Table 3. The fraction of accepted background events for those thresholds is shown in Fig. 7.

The best performance is obtained with the  $2 \times 2$  algorithm. The algorithm is not very efficient in rejecting low  $p_T$  muons, because they are accompanied by rather low energy jets. However, for muons with  $p_T$  above 15-25 GeV one can achieve an additional rejection factor of 3-10 over the nominal muon trigger.

## 5 Conclusions

The isolated muon trigger can be used to suppress the  $c\bar{c}$  and  $b\bar{b}$  background. Several algorithms have been simulated. The best performance is obtained with the algorithm based on  $2 \times 2$  calorimeter regions. It was shown that the algorithm is feasible and significant rejection factor (of the order of 3-10) can be achieved at the expense of a 5-10 % loss of the signal with respect to the muon trigger without this algorithm. Similar, but more sophisticated algorithm can also be used for the CMS High Level Triggers.

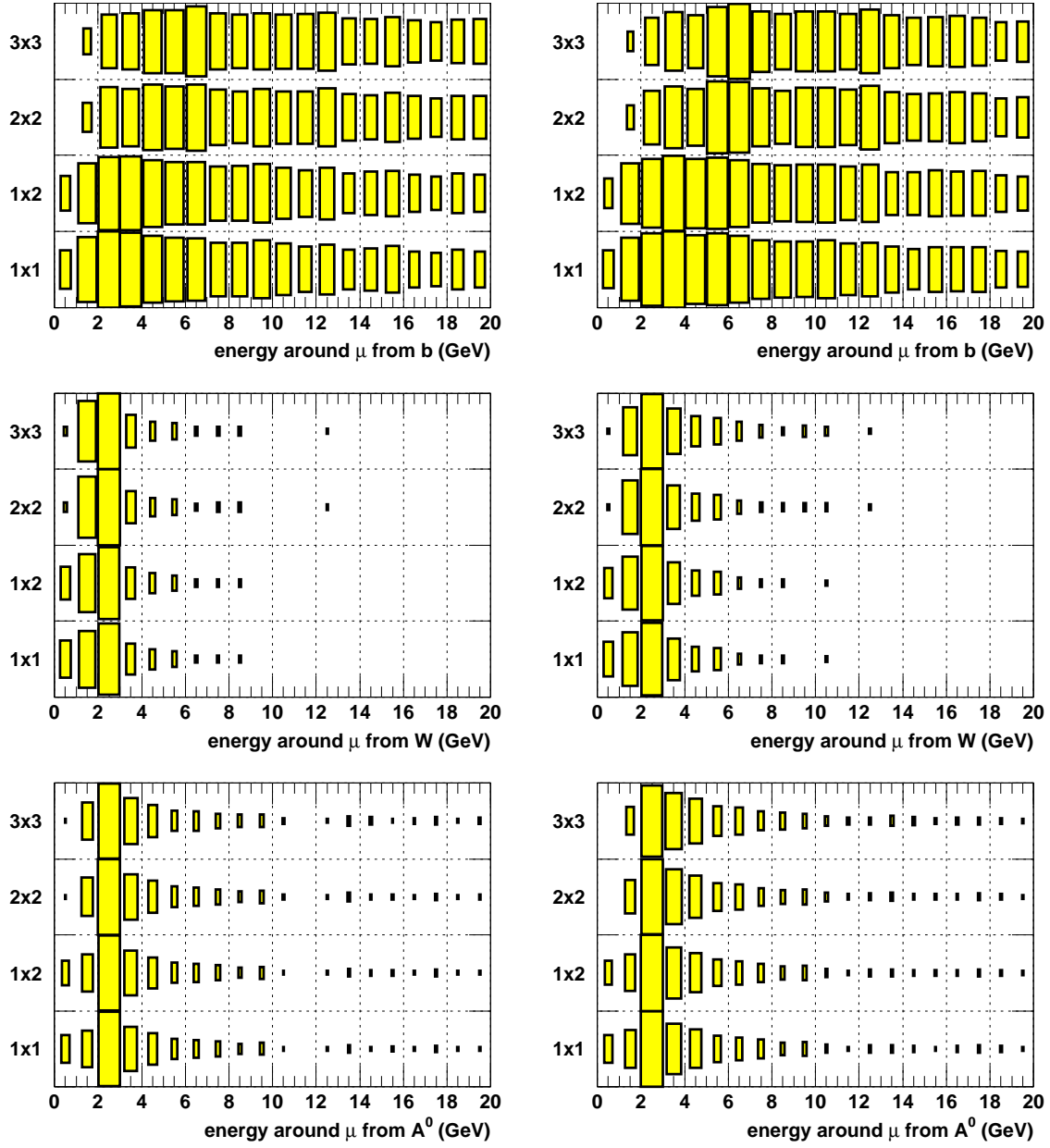


Figure 4: Distribution of energy deposited around a muon for different sizes of the isolation window at  $\mathcal{L} = 10^{33} \text{cm}^{-2} \text{s}^{-1}$  (left) and  $\mathcal{L} = 10^{34} \text{cm}^{-2} \text{s}^{-1}$  (right).

## References

- [1] CMS Bulletin 1996-01, page 14.
- [2] *PYTHIA 5.7 and JETSET 7.4 Physics and Manual*, T.Sjöstrand, **CERN-TH.7112/93**, **LU TP 95-20**  
T.Sjöstrand, *Computer Physics Commun.* **82** (1994) 74.
- [3] *CMSIM: CMS Simulation Package – Users’ Guide and Reference Manual*,  
<http://cmsdoc.cern.ch/cmsim/cmsim.html>

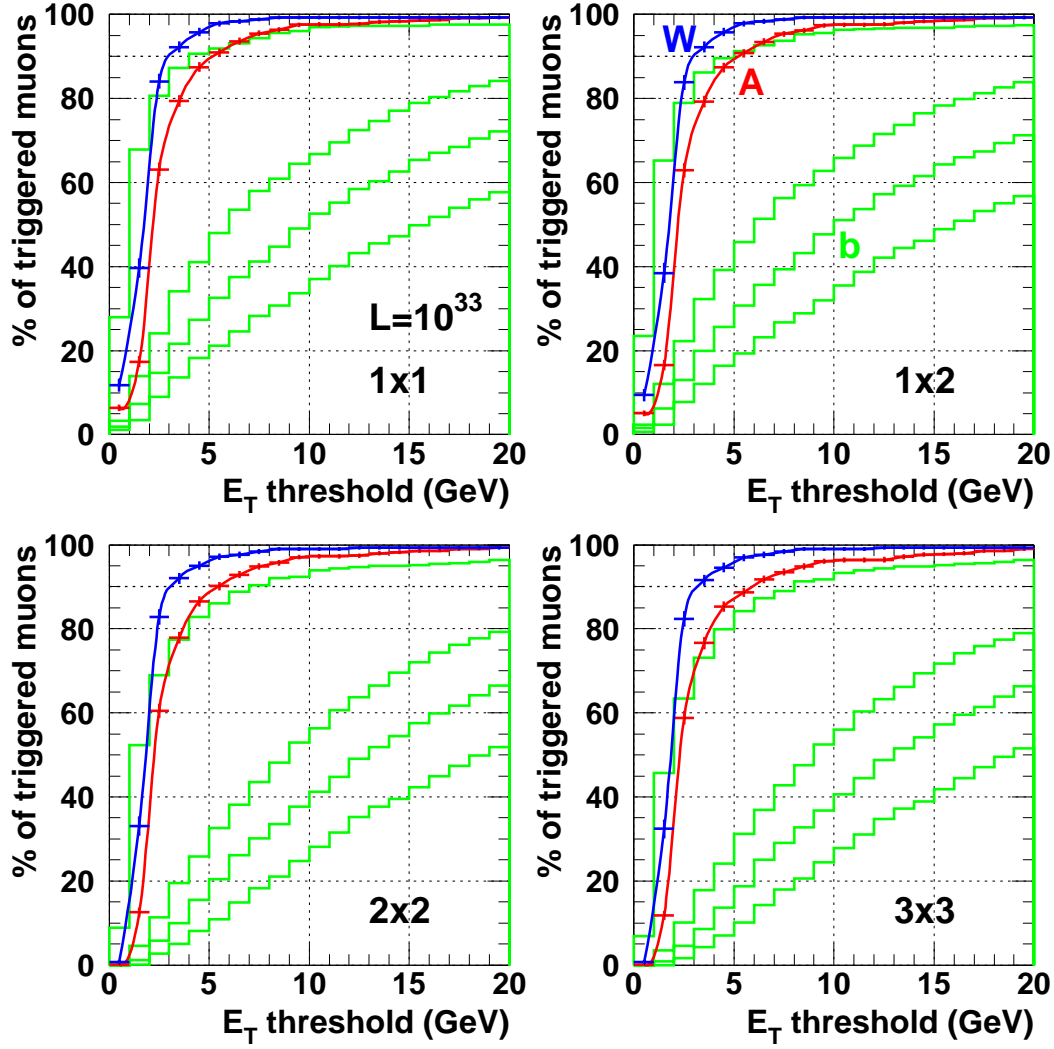


Figure 5: Fraction of accepted events as a function of energy threshold at low luminosity. The upper and lower curves with error bars represent the  $W$  and  $A^0$  signal respectively. The four histograms in each plot correspond to muons from  $b$ -quark decays with  $p_T > 5$  (the highest histogram), 15, 20 and 25 GeV.

algorithm	$\Delta\eta \times \Delta\phi$	$E_T$ threshold	
		$\mathcal{L} = 10^{33} \text{cm}^{-2} \text{s}^{-1}$	$\mathcal{L} = 10^{34} \text{cm}^{-2} \text{s}^{-1}$
$1 \times 1$	$0.35 \times 0.35$	6 GeV	7 GeV
$1 \times 2$	$0.35 \times 0.70$	6 GeV	7 GeV
$2 \times 2$	$0.70 \times 0.70$	6 GeV	7 GeV
$3 \times 3$	$1.05 \times 1.05$	7 GeV	8 GeV

Table 3: Muon isolation thresholds for different algorithms.

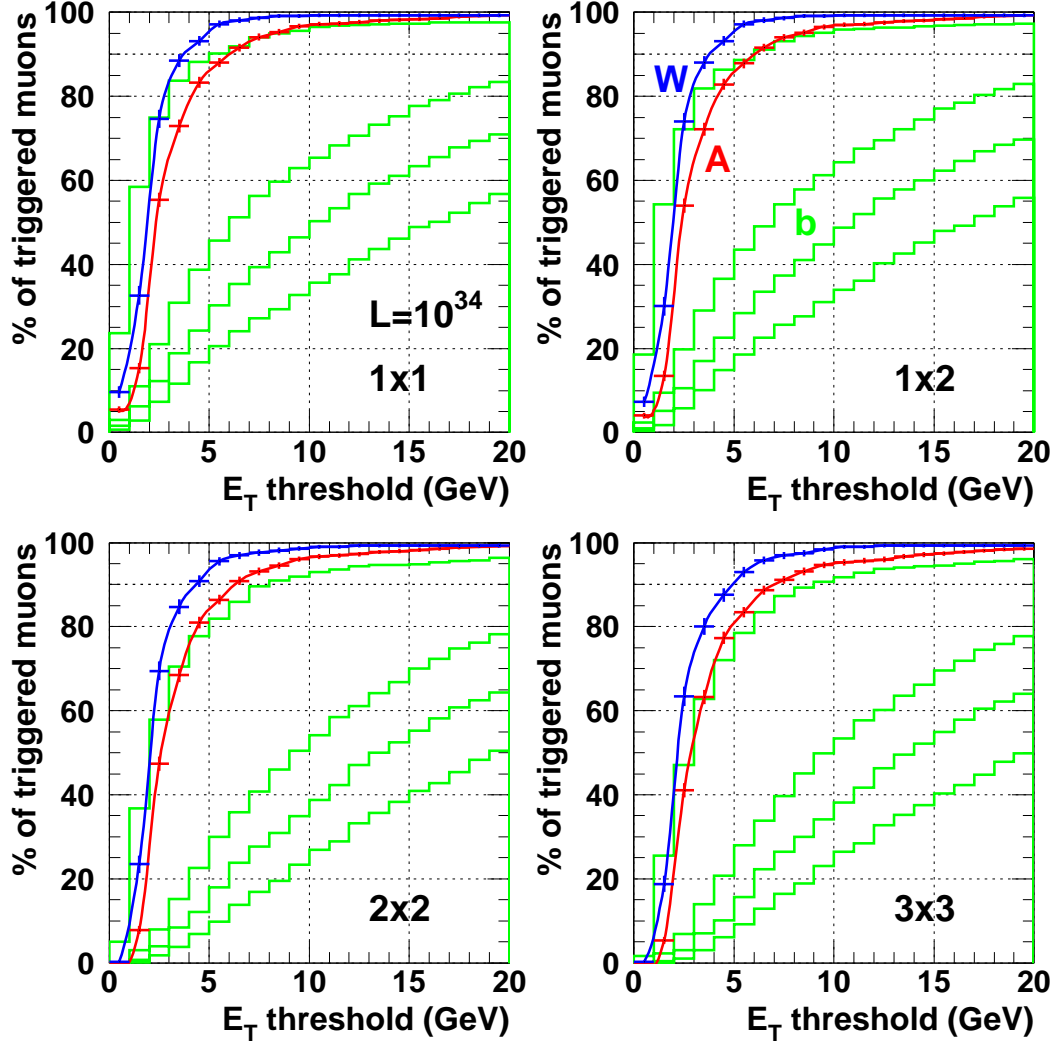


Figure 6: Fraction of accepted events as a function of energy threshold at high luminosity. The upper and lower curves with error bars represent the W and  $A^0$  signal respectively. The four histograms in each plot correspond to muons from b-quark decays with  $p_T > 5$  (the highest histogram), 15, 20 and 25 GeV.

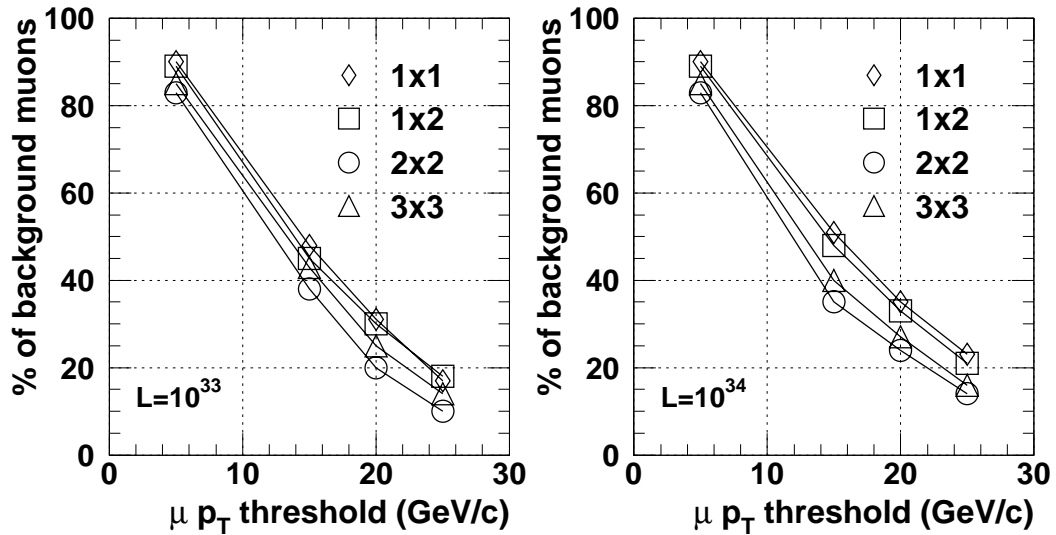


Figure 7: Fraction of accepted background events as a function of muon  $p_T$  cut.